Analysis of the December 2006 proton test data on the high-stress module and the 2006 cold performance tests on the high-stress module plus a re-analysis of the October 2005 proton test data on the low-stress module

Martin Groenewegen (ICC KUL)

DOCUMENT CHANGE RECORD

Version	Date	Changes	Remarks
Draft 0	01-January-2007	–	start of document
Draft 1	18-May-2007	all	released to PACS-ICC

Reference Documents

RD 1 – Test Plan and procedure for investigation of glitch event rate and collected charge variation in the Ge:Ga detectors during proton irradiation at UCL-CRC (4th test phase, PACS-ME-TP-009, issue 4.0, 15 November 2006, Katterloher, Barl & Royer
RD 2 – Cold performance tests on FM High-Stress Ge:Ga detector modules, PACS-ME-TR-063, issue 1, L. Barl, 10.08.2006
RD 3 – Simulations and analysis of PACS Spectrometer Ramps under irradiation conditions: impact on science goals and AOT design, PICC-KL-TN-025, draft 1, July. 2006 Groenewegen
RD 4 – Fitting PACS ramps with analytical models. Part III: The IMEC model, PICC-KL-TN-010, M.A.T. Groenewegen & P. Merken
RD 5 – Analysis of the April 2005 proton test data, PICC-KL-TN-020, draft 1, Dec. 2005 Groenewegen & Royer (KUL)
RD 6 – Analysis of the October 2005 proton test data on the low-stress module, PICC-KL-TN-024, M.A.T. Groenewegen

1. Introduction

This report focuses on the fourth phase of the proton irradiation tests which took place in the cyclotron at Louvain-La-Neuve (UCL-CRC) between 3 and 4 December 2006, and which is described in RD 1.

In addition, and as comparision, some data that was put at our disposal in March 2006 from L. Barl's cold performance tests are also analysed (see a description in RD2)

2. Model fitting of the ramps

Two different models have been fitted to the ramps, (a) a linear fit which gives a "slope", and, (b) the IMEC model of the ramps, as e.g. described in RD 4 and RD 3.

As described in the latter work, many of its free parameters can be fixed or are known (bias voltage, capacitance), and two parameters are actually fitted (like in the linear model).

One of these parameters is dubbed $R_{\rm d}$, the resistance of the detector, a proxy for the power of the in-falling infra-red light. This can be converted to a "*slope*":

$$slope = \frac{dV(t)}{dt} = \frac{-V_{\rm b}}{C_{\rm f}\ R_{\rm d}} \tag{1}$$

with $V_{\rm b}$ the bias voltage, and $C_{\rm f}$ the feedback capacitance.

In other words, $R_{\rm d}$ is fitted, and then *slope* is calculated according to Eq. 1. The advantage is that a comparison is possible with the slopes derived by fitting a straight line to the data.

3. The 2006 cold performance tests

Tables 1-3 contain the results for data from FM HS 4, file T185bb10b70t025c02n128_1 for modules 0-5, and for the 16 pixels. As Barl remarked in RD 2 that there is an important dark current which is pixel dependent, but on the other hand we had not the files at our desposal taken with no light, the signal from pixel 0 was subtracted as a first-order dark current subtraction.

Listed are the *slope*, standard deviation, the resulting (S/N), and the noise (determined by fitting a Gaussian to the residuals between the data and the fit to the data) from the fitting of the IMEC model, and then the slope and (S/N) from the fitting of a straight line.

The best (S/N) of 5140 is in module 5 pxl 4. The number of pixels per module that have a S/N better than 80% of this maximum (>4110), are module 0: 13, module 1: 7, module 2: 12, module 3: 4, module 4: 12, module 5: 15, indicating that the variation in responsivity is considerable over the modules.

Table 1: FM HS 4: T185bb10b70t025c02n128_1.dat detector zero subtracted module 0 and 1

Pxl	*slope*	STDDEV	(S/N)	noise	slope	(S/N)	*slope*	STDDEV	(S/N)	noise	slope	(S/N)
1	-2.3676	0.00876	3055	0.00130	-2.2337	3046	-2.6391	0.00617	4840	0.00117	-2.4788	5071
2	-2.0824	0.00611	3855	0.00110	-1.9739	3996	-2.4877	0.00717	3926	0.00110	-2.3423	4081
3	-2.1118	0.00562	4249	0.00115	-2.0009	4385	-2.4471	0.00691	4007	0.00127	-2.3057	4179
4	-2.1428	0.00528	4593	0.00097	-2.0292	4762	-2.3150	0.00631	4152	0.00121	-2.1860	4307
5	-2.1628	0.00534	4581	0.00098	-2.0475	4755	-2.3647	0.00676	3958	0.00117	-2.2311	4117
6	-2.1770	0.00538	4577	0.00097	-2.0605	4751	-2.4835	0.00687	4092	0.00113	-2.3386	4269
7	-2.2316	0.00582	4341	0.00113	-2.1102	4509	-2.6196	0.00728	4073	0.00142	-2.4612	4262
8	-2.2222	0.01186	2119	0.00456	-2.1018	2197	-2.6217	0.00650	4562	0.00117	-2.4631	4760
9	-2.2834	0.00520	4947	0.00101	-2.1574	5151	-2.5375	0.00670	4259	0.00127	-2.3873	4452
10	-2.3304	0.00630	4185	0.00100	-2.2000	4352	-2.4554	0.00731	3798	0.00097	-2.3133	3960
11	-2.3540	0.00520	5116	0.00100	-2.2215	5318	-2.4563	0.00775	3588	0.00117	-2.3140	3735
12	-2.3918	0.00565	4788	0.00113	-2.2557	4986	-2.5851	0.00683	4281	0.00125	-2.4302	4472
13	-2.3858	0.00608	4437	0.00113	-2.2503	4622	-2.5736	0.00734	3966	0.00142	-2.4199	4134
14	-2.4035	0.00636	4271	0.00116	-2.2662	4454	-2.4203	0.00837	3271	0.00136	-2.2814	3522
15	-2.4764	0.00608	4604	0.00121	-2.3323	4780	-2.3719	0.00609	4403	0.00117	-2.2377	4578
16	-2.7460	0.00657	4727	0.00129	-2.5745	4961	-2.6367	0.00668	4463	0.00156	-2.4766	4650

A S/N better than 90% of the maximum ($>$4626) are: module 5, pixel 16 (slope= -4.47); module 5, pixel 12 (-3.35); module 0, pixel 15 (-2.48); module 0, pixel 4 (-2.14), which all will be considered below.

In 92/96 cases the S/N from the slope-fitting is higher than that from IMEC-model, by 3-5%. The free parameters in the IMEC model have not been optimised w.r.t. the values derived in RD 5 for the April 2005 proton test data, but on the other hand it seems clear that fitting a straight line is a good measure of the flux.

In Table 4 the results are shown for the four best pixels as a function of bias voltage. The results indicate that the best S/N are achieved for 70 mV, with 60 mV a good second.

Table 5 shows the results for 2 pixels for diffenent bias voltages and capacitance values. This confirms the conclusion above: the highest S/N are achieved for bias= 70 mV and c= 0.2 pF, closely followed by bias= 60 mV where c= 0.1 pF gives better results than 0.2 pF on some pixels.

The power on the pixel for a BB temperature of 10 K is 1.0 E(-14) W (RD 2). This results in a current of: I = C $\frac{dV}{dt}$ = 230 E(-15) $\times$ 2.4764 = 5.70 E(-13) A, and therefore a responsivity of 57 A/W, in line with the results quoted in RD 2.

In the Tables the S/N is defined median(slopes)/stddev(slopes) * $\sqrt{n\_ramps}$, while in Sect 5.4 of RD 2: NEP= $\sqrt{2\, t\_int}$ Flux / (median(slopes)/stddev(slopes)). From this we derive an NEP of 1.7 E(-17), in line with results in RD 2.

3. December 2006 proton test data

Table 6 presents the slope and S/N calculation for all pixels for a pre-beam file. Pixels 1,2,4,5 are "Akari" pixels and should not be considered here.

Examples of pixels with poor, average, good S/N are, respectively, pixel 11,12,13, and for these (and pixel 0) we have analysed the time series T185b30t025c02n256_fl035_L_1 through L_45 for a total duratiopn of about 3 hours. The results are shown in Fig. 1, and illustrate the dramtically different behaviour between pixels. Whereas pixel 11 and 12 seem to have reached a plateau, this is not the case for pixel 13.

After the 3h irradiation data was taken for different biases and capacitance values, and the results for pixels 11,12,13 are listed in Table 7. There is no nicely defined maximum as in the case of the pre-beam data, but considering these 3 pixels, bias values of 30-40 mV and capacitance value 0.1-0.2 pF bracket the best S/N.

Table 2: FM HS 4: T185bb10b70t025c02n128_1.dat detector zero subtracted module 2 and 3

Pxl	*slope*	STDDEV	(S/N)	noise	slope	(S/N)	*slope*	STDDEV	(S/N)	noise	slope	(S/N)
1	-2.6227	0.00665	4465	0.00166	-2.4640	4669	-1.5252	0.00400	4313	0.00083	-1.4594	4422
2	-2.3692	0.00641	4181	0.00120	-2.2352	4350	-1.3090	0.00406	3644	0.00091	-1.2571	3725
3	-2.2889	0.00590	4372	0.00113	-2.1623	4538	-1.3203	0.00400	3728	0.00102	-1.2677	3822
4	-2.3131	0.00601	4353	0.00113	-2.1843	4538	-1.2655	0.00370	3871	0.00099	-1.2160	3953
5	-2.2630	0.00519	4933	0.00112	-2.1388	5122	-1.3437	0.00384	3952	0.00097	-1.2895	3885
6	-2.2959	0.00581	4452	0.00121	-2.1597	4628	-1.3602	0.00399	3846	0.00102	-1.3050	3934
7	-2.3944	0.00628	4315	0.00128	-2.2580	4494	-1.3771	0.00409	3807	0.00099	-1.3209	3900
8	-2.4463	0.00705	3927	0.00121	-2.3051	4095	-1.3673	0.00434	3563	0.00093	-1.3116	3649
9	-2.5612	0.00621	4666	0.00127	-2.4086	4875	-1.3604	0.00403	3802	0.00084	-1.3052	3902
10	-2.5184	0.00605	4707	0.00091	-2.3701	4912	-1.3999	0.00374	4239	0.00077	-1.3423	4340
11	-2.4898	0.00574	4909	0.00104	-2.3444	5123	-1.3969	0.00409	3865	0.00084	-1.3394	3952
12	-2.3495	0.00713	3729	0.00636	-2.2174	3944	-1.4278	0.00401	4024	0.00097	-1.3683	4119
13	-2.2948	0.00627	4140	0.00116	-2.1678	4301	-1.4516	0.00427	3847	0.00105	-1.3907	3943
14	-2.3364	0.00655	4033	0.00121	-2.2054	4190	-1.4095	0.00379	4207	0.00097	-1.3512	4320
15	-2.4222	0.00717	3821	0.00127	-2.2833	3970	-1.4949	0.00395	4276	0.00097	-1.4311	4402
16	-2.8661	0.00753	4303	0.00129	-2.6819	4515	-1.7139	0.00606	3195	0.00193	-1.6347	3286

4. Simulated chopping

In this section the results on "simulated chopping" are described. The long timeseries L1-L45 is considered preceded by the three pre-beam files taken with the same bias voltage and capacitance: T185b30t025c02n256_fl035_#N_15, T185b30t025c02n1680_fl035-0375-035_#N_32.dat, T185b30t025c02n1680_fl035-043-035_#N_33.

We consider the SED-mode like AOT, i.e 2 ramps per chopper plateau, 2 chopper cycles, up-and-down scan, 1 nod cycle. In RD 3 we considered that every line is seen by 2 pixels, here we consider the more realistic case were every line is seen–on average–by 2.5 pixels. Therefore a line is seen by 40 ramps (on-source). In reality these are not consecutive, but here we will consider batches of 80 consecutive ramps, 2 off, 2 on, 2 off, etc.

The slopes of the 'on' ramps are multiplied by an arbitrary factor 1.06 (to simulate we are observing a source 6% of the background).

To every set of 40 off-source ramps a spline is fitted, after removing 3-sigma outliers. At this point a more sophisticated deglitching algortithm on the slopes could also be employed.

Many other possibilities than spline fitting can be considered (linear interpolation using the offs around a on; low-order polynominal). Experimentially it was found that with 40 values, 6 knots for the spline give good results. Figure 2 illustrates the procedure for pixel 11, chosen for illustration as it reaches the responsivity plateau, contrary to the other pixels.

The spline is then used to estimate the background at the location of the on-s, and the on-source are then divided by the estimated off-source slopes. The bottom left panel of Figure 2 shows the distribution. At this point 3-sigma outliers are removed. Again a deglitching algorithm on the on-source slopes could also have been used.

Of this distribution the median, and the precision on the median (calculated as stddev/$\sqrt{n}$, with n typically 40 unless a few outliers have been removed) are determined.

Another procedure was also employed. A histogram of the distribution of fluxes was made (using 5 bins), and to this distribution a Gaussian was fitted (see bottom right panel in Figure 2). Output values from this procedure are the mean of the Gaussian, the error in the mean, and the sigma value associated with the width of the Gaussian.

Figure 3 show how these different quantities vary as a function of time over the 3h irradiation test. The surpsising result is that the noise properties do not degrade as the irradiation proceeds. Also the input flux of 1.06 $\times$ background is recovered without bias.

Table 3: FM HS 4: T185bb10b70t025c02n128_1.dat detector zero subtracted module 4 and 5

Pxl	*slope*	STDDEV	(S/N)	noise	slope	(S/N)	*slope*	STDDEV	(S/N)	noise	slope	(S/N)
1	-2.8134	0.00765	4160	0.00150	-2.6348	4366	-2.8691	0.00910	3550	0.00125	-2.6845	3726
2	-2.4368	0.01228	2245	0.00178	-2.2965	2338	-2.2908	0.00614	4219	0.00098	-2.1642	4378
3	-2.3397	0.00658	4023	0.00119	-2.2085	4183	-2.4907	0.00555	5075	0.00116	-2.3452	5301
4	-2.2293	0.00596	4228	0.00117	-2.1082	4387	-2.6114	0.00575	5140	0.00117	-2.4539	5382
5	-2.3646	0.00599	4463	0.00115	-2.2311	4649	-2.6481	0.00696	4302	0.00133	-2.4870	4302
6	-2.4007	0.00605	4489	0.00119	-2.2638	4670	-2.7463	0.00636	4881	0.00140	-2.5749	4881
7	-2.3555	0.00544	4894	0.00110	-2.2229	5102	-2.9378	0.00774	4294	0.00175	-2.7456	4513
8	-2.2750	0.00563	4574	0.00105	-2.1497	4758	-3.0749	0.00693	5023	0.00192	-2.8674	5289
9	-2.2216	0.00524	4792	0.00101	-2.1012	4976	-3.0894	0.00742	4707	0.00158	-2.8803	4968
10	-2.2139	0.00556	4508	0.00094	-2.0941	4679	-3.1416	0.00757	4693	0.00162	-2.9265	4953
11	-2.2355	0.00768	3292	0.00101	-2.1137	3414	-3.3621	0.00852	4464	0.00111	-3.1207	4727
12	-2.1258	0.00582	4132	0.00103	-2.0137	4281	-3.3547	0.00813	4666	0.00164	-3.1140	4942
13	-2.0532	0.00559	4158	0.00105	-1.9473	4300	-3.1737	0.00789	4539	0.00163	-2.9547	4800
14	-2.0492	0.00510	4547	0.00104	-1.9436	4699	-3.4658	0.00860	4564	0.00171	-3.2112	4836
15	-1.9782	0.00488	4589	0.00107	-1.8784	4737	-3.5389	0.00832	4807	0.00158	-3.2752	5107
16	-2.4232	0.01637	1675	0.00148	-2.2844	1745	-4.4707	0.01101	4595	0.00212	-4.0754	4956

Table 4: FM HS 4, T185bb10b??t025c02n128_1.dat, detector zero subtracted. mod 5 pxl 16 (top left-hand); mod 5 pxl 12 (top right-hand) mod 0 pxl 15 (bottom left-hand); mod 0 pxl 4 (bottom right-hand)

Bias	*slope*	STDDEV	(S/N)	noise	slope	(S/N)	*slope*	STDDEV	(S/N)	noise	slope	(S/N)
90												
80							-5.2515	0.02329	2550	0.00500	-4.7772	2571
70	-4.4707	0.01100	4595	0.00212	-4.0754	4956	-3.3546	0.00813	4666	0.00164	-3.1140	4942
60	-2.8691	0.00590	5431	0.00111	-2.6637	5747	-2.1782	0.00526	4688	0.00096	-2.0492	4888
50	-1.8481	0.00512	4080	0.00107	-1.7374	4269	-1.3821	0.00515	3022	0.00079	-1.3134	3131
40	-1.1031	0.00369	3378	0.00098	-1.0484	3478	-0.8183	0.00286	3233	0.00077	-0.7842	3334
90	-5.7144	0.09039	328	0.00690	-5.2101	354	-4.7595	0.04730	965	0.01180	-4.3923	1027
80	-3.7958	0.01523	2818	0.00305	-3.5252	2981	-3.1968	0.01211	2985	0.00204	-2.9946	3127
70	-2.4764	0.00608	4604	0.00121	-2.3323	4780	-2.1428	0.00528	4593	0.00098	-2.0292	4762
60	-1.6394	0.00410	4528	0.00095	-1.5585	4675	-1.4282	0.00430	3761	0.00092	-1.3634	3888
50	-1.0545	0.00336	3546	0.00092	-1.0099	3633	-0.9173	0.00349	2969	0.00095	-0.8813	3031
40	-0.6316	0.00332	2150	0.00089	-0.6085	2185	-0.5497	0.00272	2287	0.00096	-0.5309	2342

Comparing the top-right with the middle-left panel shows that calculating the precision in the mean simply from the standard deviation is more robust than fitting a Gaussian to the distribution.

The influence of the length of the chopper plateau is also investigated. Table 8 shows that the best results are achieved for 1 or 2 ramps per chopper plateau. With longer chopper plateaus the precision on the mean becomes worse which is related to how accurate the background at the on-positions can be determined by interpolation [altough this in part is related to the nature of the spline-fitting].

It should be pointed out that data files were taken with 0.25s ramps while in SED-mode ramps with 1/8s will be taken. In addition, the onboard software can do either of two things: derive a slope from the 32 NDRs, or down-link the average of the first and second batch of 16 NDRs (from which a slope can be derived on-ground).

Both methods are compared to the result with slope-fitting to 64 NDRs in Table 8. There is little difference between the 2 methods, and the precision in both are approximately a factor 1.3 worse than with ramps of 1/4sec.

There are 3 estimates of the noise: the mean value of the Gaussian fit to the distribution of precisions, the median value of

Table 5: FM HS 4, T185bb10b?0t025c??n128_1.dat. Detector zero subtracted. mod 0 pxl 15 (left); mod 0 pxl 4 (right)

Bias	*slope*	STDDEV	(S/N)	noise	slope	(S/N)	*slope*	STDDEV	(S/N)	noise	slope	(S/N)
b70 c01	-4.1073	0.01200	3857	0.00234	-3.7662	4127	-3.5605	0.00095	4218	0.00190	-3.2942	4480
b70 c02	-2.4764	0.00608	4604	0.00121	-2.3323	4780	-2.1428	0.00528	4593	0.00098	-2.0292	4762
b70 c04	-1.2843	0.00377	3849	0.00089	-1.2337	3920	-1.1037	0.00375	3325	0.00084	-1.0636	3391
b70 c11	-0.5098	0.00173	3339	0.00084	-0.4961	4675	-0.4353	0.00162	3043	0.00083	-0.4242	3028
b70 c01	-4.1073	0.01200	3857	0.00234	-3.7662	4127	-3.5605	0.00095	4218	0.00190	-3.2942	4480
b60 c01	-2.7138	0.00703	4365	0.00118	-2.5275	4598	-2.3738	0.00616	4361	0.00111	-2.2249	4587
b50 c01	-1.7428	0.00509	3873	0.00102	-1.6424	4031	-1.5268	0.00488	3540	0.00103	-1.4461	3668
b60 c02	-1.6394	0.00410	4528	0.00095	-1.5585	4675	-1.4282	0.00430	3761	0.00092	-1.3634	3888
b80 c04	-1.9693	0.00880	2530	0.00121	-1.8779	2607	-1.6523	0.00642	2911	0.00091	-1.5831	2987
b90 c04	-2.9601	0.04331	773	0.00477	-2.7953	804	-2.4598	0.02826	984	0.00220	-2.3381	1016
b90 c11	-1.1812	0.01778	751	0.00117	-1.1416	763	-0.9736	0.01229	822	0.00094	-0.9436	833

the precisions, and the width of the Gaussian fit to the distribution of flux ratio's. The poorest value of 0.001743 is taken.

Taking the telescope background equivalent point source flux from AlPog's latest Instrument Model at the wavelength of the highest S/N (In first order 1132 Jy at 132 μm), this corresponds to a 1-sigma flux density of 2.0 Jy at 132 μm.

The expected 1-sigma noise values for the SED-mode (40 ramps of 1/8s = 5 sec and off-array chopping) is 0.41 Jy.

This indicates that the "fudge-factor" of 1.2 adopted in HSPOT version 2.0 is underestimated. A calculatation as a function of wavelength indicates that in the range 110-210 micron this factor is typically 4.0.

7. Re-analysis of Low-stress data

The simulated chopping analysis has also been carried out on the proton-test data taken on the low-stress module in october 2005 (see RD 6, and issue 3.1 of RD 1).

The following sequence of files was used: T25b120t025c14n1024_#L_94, L_97, L_100 - 112, L_115

It should be noted that better (S/N) values can be achieved at lower bias and lower capacitance values than the 120 mV, 1.42 pF taken in the actual observations.

Table 9 and Figure 4 show the results for pixel 3. As the bias and capacitance values are not optimal we take in this case the best value of 37.E-4 as the 1-sigma uncertainty in the flux determination.

Taking the telescope background equivalent point source flux from AlPog's latest Instrument Model at the wavelength of the highest S/N (1815 Jy at 60 μm, 1402 Jy at 76 μm), this corresponds to a 1-sigma flux density of 6.7 Jy at 60 μm, and 5.2 Jy at 76 μm.

The expected 1-sigma noise values for the SED-mode (40 ramps of 1/8s = 5 sec and off-array chopping) are, respectively: 2.14, and 1.19 Jy.

This indicates that the "fudge-factor" of 1.2 adopted in HSPOT version 2.0 is underestimated. A calculatation as a function of wavelength indicates that in the range 55-70 micron this factor is typically 2.4, in the range 72-96 micron typically 2.9.

Table 6: FM HS 185: T185b30t025c02n256_fl035_N_15.dat. Detector zero NOT subtracted. Pixels 1,2,4,5 are "Akari" pixels and are listed for completeness only.

Pxl	*slope*	STDDEV	(S/N)	noise	slope	(S/N)
0	-0.0013	0.00141	13	0.00078	-0.0011	9
1	-2.0852	0.00855	3901	0.00105	-1.8163	4210
2	-2.9135	0.01016	4585	0.00136	-2.4663	5100
3	-0.2824	0.00316	1427	0.00097	-0.2625	1438
4	-3.9648	0.01511	4198	0.00130	-3.2384	4837
5	-2.7583	0.01129	3909	0.00114	-2.3472	4312
6	-0.3640	0.00348	1672	0.00097	-0.3372	1698
7	-0.5185	0.00343	2407	0.00097	-0.4771	2455
8	-0.4036	0.00344	1875	0.00093	-0.3734	1908
9	-0.3876	0.00334	1853	0.00096	-0.3588	1884
10	-0.4043	0.00336	1922	0.00095	-0.3741	1957
11	-0.6395	0.00402	2541	0.00098	-0.5864	2596
12	-0.3983	0.00340	1872	0.00095	-0.3687	1897
13	-0.3410	0.00336	1635	0.00098	-0.3162	1658
14	-0.3118	0.00354	1408	0.00100	-0.2894	1417
15	-0.4318	0.00358	1926	0.00100	-0.3991	1958
16	-0.3917	0.00364	1717	0.00100	-0.3626	1742

Table 7: FM HS 185: at plateau, different bias and capacitance settings for 3 different pixels (11, 12, 13, respectively). Detector zero NOT subtracted

	slope	STDDEV	(S/N)	*slope*	STDDEV	(S/N)	*slope*	STDDEV	(S/N)
L49= bb50 c02	-17.092	0.2709	890	-7.3483	0.2173	541	-6.1828	0.0465	2129
L54= bb40 c02	-10.005	0.2064	775	-3.9414	0.0438	1438	-3.7172	0.0348	1707
L59= bb30 c02	-4.7279	0.0846	891	-2.0641	0.0304	1083	-1.9040	0.0148	2052
L67= bb20 c02	-2.0106	0.0387	830	-1.0259	0.0417	393	-0.7731	0.0102	1218
L72= bb10 c02	-0.5591	0.0103	866	-0.3114	0.0071	700	-0.2304	0.0046	799
L62= bb30 c01	-8.4602	0.1314	1011	-3.6672	0.0450	1301	-3.3165	0.0210	2532
L59= bb30 c02	-4.7279	0.0846	891	-2.0641	0.0304	1083	-1.9040	0.0148	2052
L63= bb30 c04	-2.2392	0.0311	1153	-1.0705	0.0157	1088	-0.9745	0.0103	1538
L64= bb30 c10	-0.8558	0.0112	1224	-0.4032	0.0080	809	-0.3762	0.0038	1580

Table 8: Simulated Chopping exercise for pixel 11. First column lists Ramps per chopper plateau and number of chop cycles per line.

chopping	precision mean Gauss.	precision width Gauss.	precision median	Flux mean Gauss.	Flux width Gauss.	comment
1 – 40	8.85E-4	2.42E-4	9.29E-4	1.0600	0.001459	1/4s, slope from 64 NDRs
2 – 20	9.27E-4	2.39E-4	9.76E-4	1.0600	0.001275	1/4s, slope from 64 NDRs
4 – 10	11.04E-4	4.32E-4	11.77E-4	1.0599	0.001436	1/4s, slope from 64 NDRs
5 – 8	12.37E-4	5.16E-4	12.88E-4	1.0600	0.001416	1/4s, slope from 64 NDRs
8 – 5	19.82E-4	11.84E-4	24.25E-4	1.0598	0.002404	1/4s, slope from 64 NDRs
2 – 20	11.66E-4	2.94E-4	12.14E-4	1.0600	0.001741	1/8s, slope from 32 NDRs
2 – 20	12.06E-4	2.78E-4	12.47E-4	1.0599	0.001743	1/8s, slope from average of NDRs 1-16 and 17-32
2 – 20	9.96E-4	3.03E-4	10.93E-4	1.0600	0.001351	1/4s, slope from 64 NDRs, 32 ramps [not 40]

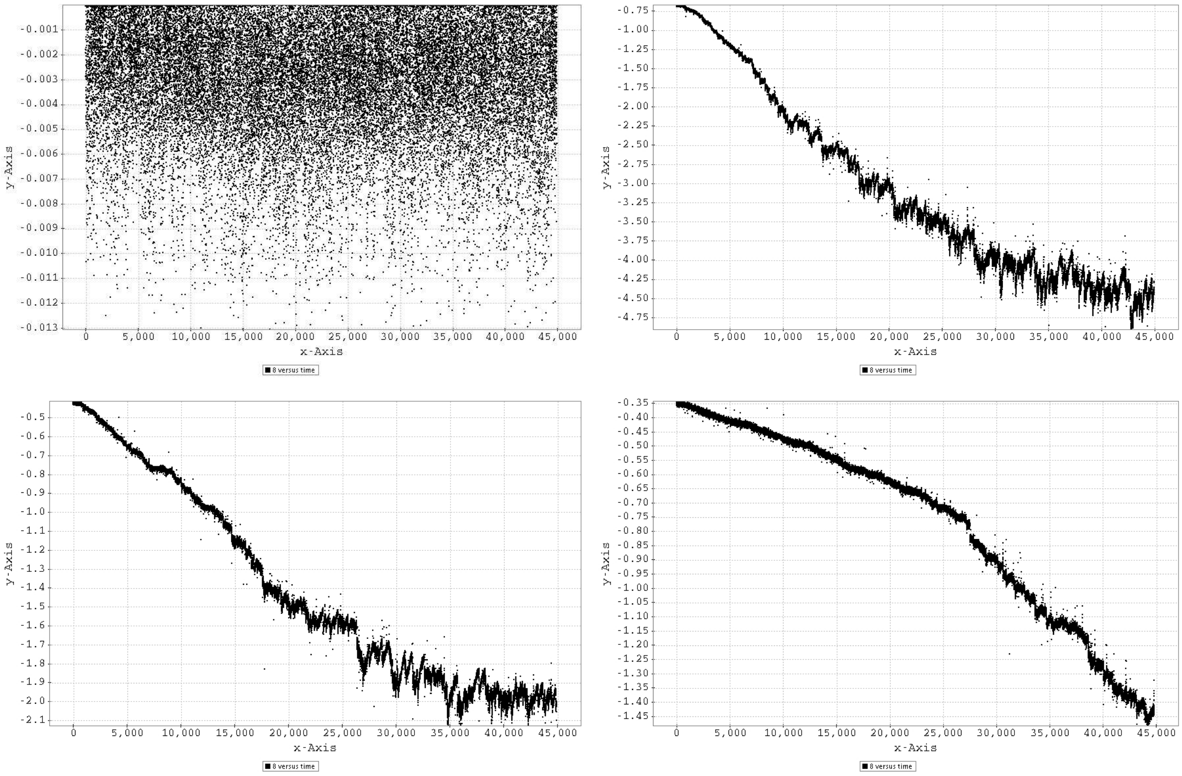

Figure 1: Slope (V/s) versus consecutive ramp number for (from left to right, top to bottom) detector 0, 11, 12, 13 of the 3 hour time series L1 to L45.

Table 9: Simulated Chopping exercise for pixel 3 of the Low-stress module. First column lists Ramps per chopper plateau and number of chop cycles per line.

chopping	precision mean Gauss.	precision width Gauss.	precision median	Flux mean Gauss.	Flux width Gauss.	comment
2 – 20	36.59E-4	16.41E-4	38.17E-4	1.0615	0.004308	1/8s, slope from 32 NDRs
2 – 20	37.10E-4	15.94E-4	38.23E-4	1.0616	0.004299	1/8s, slope from average of NDRs 1-16 and 17-32

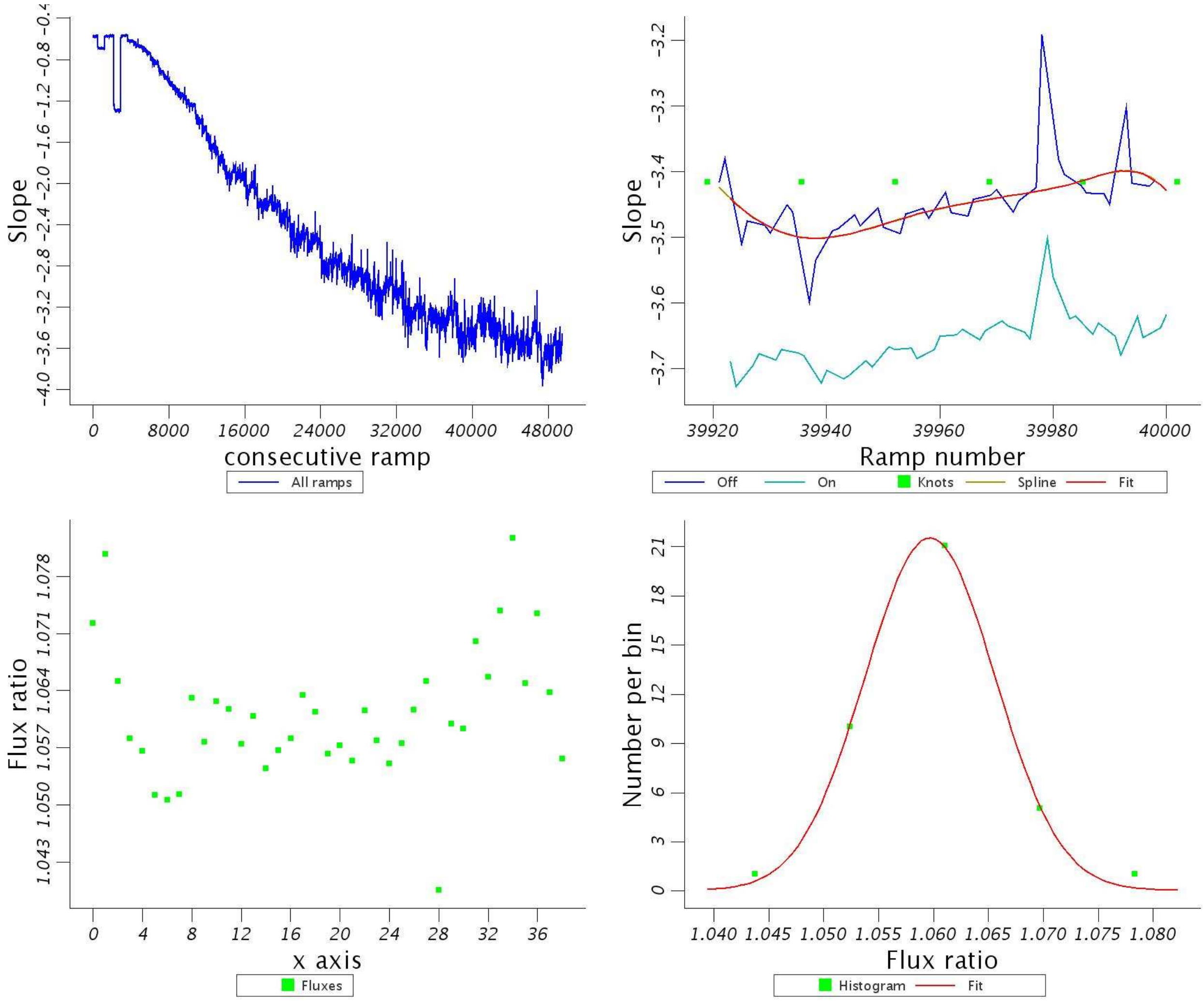

Figure 2: Procedure of "simulated chopping". Slopes of all ramps from pixel 11, including some pre-beam data (top left). A batch of 80 slopes, 2 off, 2 on, 2 off, etc. On-source slopes are multiplied by 1.06. A spline with 6 knots is fitted to the off-source ramps (top right). The spline is used to estimate the background at the on-source ramps, and the on-source is divided by the estimated off-source (bottom left). A histogram is made to this ratio, and a Gaussian is fitted to it (bottom right).

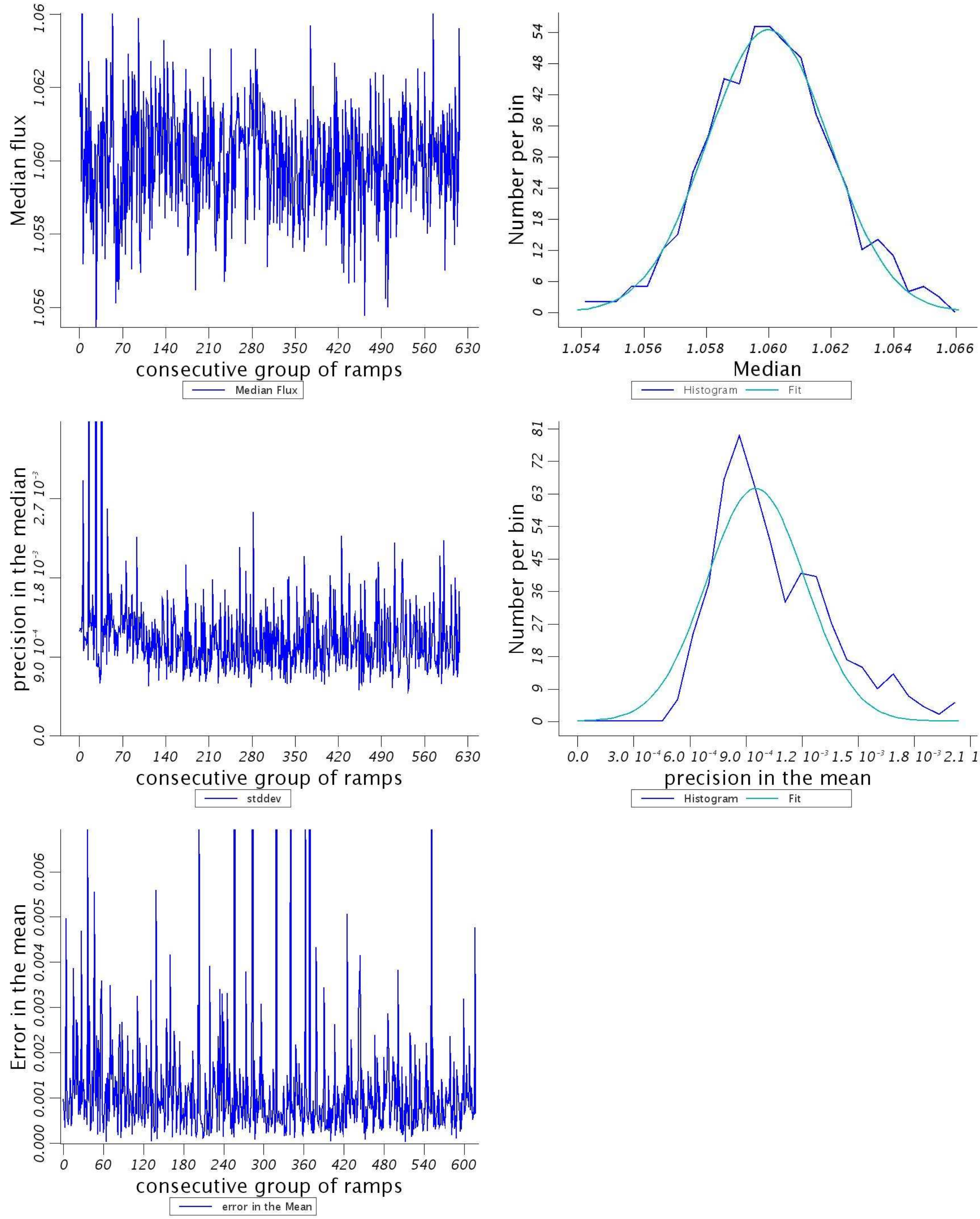

Figure 3: Top left: Median Flux; Top right: Distribution of the median (and a Gaussian fit to it, see Table 8); Middle Left: precision on the Median flux; Middle right: Distribution of the precision in the median (and a Gaussian fit to it, see Table 8); Bottom left: Error in the Mean of the Gaussian fit. Two histograms are not based on all data, but “group” 200 and later.

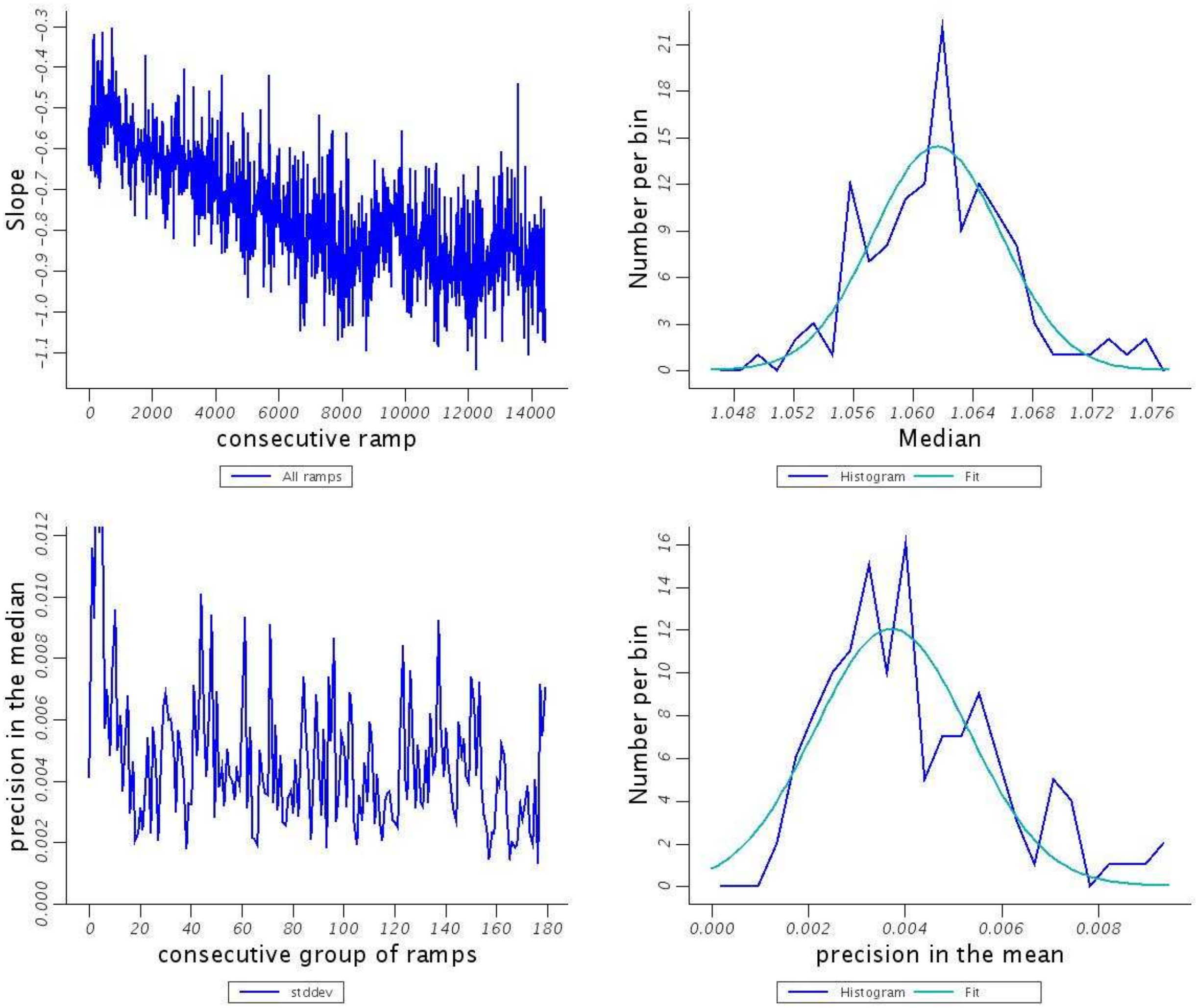

Figure 4: Top left: All ramps of pixel 3 of the low-stres smodule; Top right: Distribution of the median (and a Gaussian fit to it, see Table 8); Bottom Left: precision on the Median flux; Bottom right: Distribution of the precision in the median (and a Gaussian fit to it, see Table 8); Two histograms are not based on all data, but “group” 50 and later.

8. Conclusions

1. Under irradiation conditions the best S/N values are achieved for bias values in the range 30-40 mV and capacitance values in the range 0.1-0.2 pF for the high-stress module.

2. There seems to be no need for (frequent) curing as the precision with which the mean of a set of slopes can be determined does not vary with the duration of the irradiation (on timescale of $\lesssim$3 hours in any case).

3. The best results are achieved with chopper plateaus of 1 or 2 ramps.

4. For ramps of 1/4s, with slope fitting to 64 NDRs, and 40 ramps per line, a precision in the mean of about 14 10^{-4} can be achieved.

   For ramps of 1/8s (appropriate for SED-mode), a precision in the mean of about 17 10^{-4} can be achieved. The results are essentially identical when the slopes are not derived from a fit to the 32 NDRs, but from the average of NDRs 1-17, and 17-32.

5. From analysis of the December 2006 and October 2005 data on the low- and high stress module, and for SED-mode operations as currently foreseen, it is estimated that a 1-sigma flux density of 6.7 Jy at 60 μm, 5.2 Jy at 76 μm and 2.0 Jy at 132 μm can be achieved.

   Averaged over the wavelength domain per order this a factor 2.4-4.0 poorer than comes out of the PACS Spectrometer Instrument model, and indicates that the currently adopted fudge factor for radiation effects of 1.2 is underestimated.

   This analysis, and hence the sensitivity estimates, do assume: (1) perfect flat-fielding between the different pixels that see a line, (2) no effects of transients, i.e. all (i.e. the 2) ramps per chopper plateau can be used.